THE NATURE AND VELOCITY OF THE SOURCES OF TYPE II SOLAR RADIO BURSTS

By THE LATE A. A. WEISS*

[*Manuscript received November* 23, 1964]

Summary

Velocities of the sources of type II bursts are derived from rates of frequency drift using standard density models, both statistically for 21 bursts, and individually for 5 bursts extending over wide frequency ranges. The derived velocities exceed the speed of sound in the magnetic-field-free corona: *on the average* the velocity decreases with increasing height to a minimum of ~ 750 km/s at a little below 1 $R_{\odot}$, and thereafter slowly increases with height. The nature of the type II source is discussed in relation to these velocities, and also in relation to detailed measurements of harmonic ratios and band splitting for the five individual bursts. It is suggested that the type II source is either a strong parallel shock (direction of propagation of shock parallel to magnetic field) or a perpendicular shock. Magnetic field strengths of 2–20 G at $0 \cdot 5$ $R_{\odot}$ above the photosphere, decreasing to 1–10 G at 2 $R_{\odot}$, are derived. Finally, it is shown that theories by which fundamental emission arises in front of the shock, whilst harmonic emission originates in the interior of the shock, are untenable.

I. INTRODUCTION

Although the solar radio burst of spectral type II has been recognized as a distinct type for nearly 15 years, the precise nature of the exciting disturbance is still unknown. Considerable attention has been given in recent years to the hypothesis that the disturbance is a shock front generated by a flare explosion and propagating along a coronal streamer, and since the corona is pervaded by magnetic fields, such a shock may well be magnetohydrodynamic (Westfold 1957; Uchida 1960; Tidman 1962). Also a magnetic origin for one of the characteristic structural features of type II bursts, namely band splitting, has been explored (Roberts 1959; Sturrock 1961). The question of the validity of these magnetic theories for the type II source is important since, if they prove to be well founded, observations of type II bursts will enable us to estimate magnetic field strengths high in the corona, in regions hitherto inaccessible to optical observation.

In the present paper we attempt to infer the nature of the type II disturbance and to estimate coronal magnetic field strengths. For this purpose we shall discuss the velocities of the sources (deduced from frequency drift rates using standard coronal density models) and also harmonic ratios and band splitting. Although much of the discussion is statistical, the conclusions are checked by appeal to several outstanding individual bursts covering wide frequency ranges. The bursts used were observed between 1952 and 1963 with the Dapto dynamic spectrograph. Because of the very low frequency limit of the Dapto spectrograph (now 5 Mc/s) we have been able to extend the observational domain to considerable heights in the corona, into

* Division of Radiophysics, CSIRO, University Grounds, Chippendale, New South Wales. Dr. Weiss died on December 30, 1964.

regions not adequately covered by the previous surveys. Statistical data for type II bursts have already been presented by Roberts (1959) and by Maxwell and Thompson (1962), but these authors did not extend their discussions to the probable shock structure of the disturbance.

II. Observations

(a) *Statistical Treatment of Drift Rates*

Measurements of the rate of frequency drift were made on any features of a burst that showed a well-defined slope, including zero. Hence the sample includes not only bursts whose main bands are well defined over a substantial frequency range, but also many short-lived individual features of complex bursts that often show quite different drift rates from one feature to the next. In all, the sample comprises 230 measurements on 21 bursts. Where convenient, measurements were made on the low frequency edges, but the ridge of maximum intensity was used when this would improve the reading accuracy. Fundamental and second harmonic bands were measured separately; in fact, considerable attention was paid to harmonic bands in an endeavour to extend the measurements to the highest possible heights in the corona. Harmonic data were reduced to fundamental bands assuming a harmonic ratio of two.

Individual drift rates are plotted in Figure 1. The tendency of drift rates to increase with frequency is very similar to that found by Maxwell and Thompson (1962), whose average relations are reproduced in the diagram. In absolute value, the Dapto drift rates appear, on the average, to be some 60% lower than those given by Maxwell and Thompson. Discussions with Dr. Maxwell suggest that differences in sampling and measuring techniques could well account for most of the discrepancy. The scatter in the individual points of Maxwell and Thompson is also similar to ours and, in agreement with them, we consider not that the scatter is due primarily to difficulties of measurement (which should not be underestimated, however) but rather that it reflects the tendency for individual features in complex bursts to have very different drift rates at nearby frequencies, and for large physical variations to occur between different bursts.

(b) *Source Velocities* (*Statistical*)

The considerations involved in the derivation of source velocities from the measured drift rates using standard density models of the corona, and in the choice of density models, have been discussed by Roberts (1959) and by Maxwell and Thompson (1962). Here, however, we wish to emphasize that the use of an average radial* electron density gradient can lead to large errors in the velocities for individual disturbances, as there are undoubtedly large fluctuations in coronal density between the streamers, where the type II sources are presumed to propagate, and in many cases the sources do not propagate even approximately radially (Weiss 1963). It is also emphasized that there are no reliable radio or optical measurements of electron

* "Radial" is used throughout this paper in the "heliocentric" rather than the "geocentric" sense.

density above active regions, at heights exceeding 1 $R_{\odot}$ above the photosphere (equivalent frequency ~ 50 Mc/s), and that above this height reliance must be placed on extrapolation of the better-known gradients at lesser heights.

With these reservations, we proceed to compute source velocities from the frequency drift rates of Figure 1. The computed quantities, which we may term the

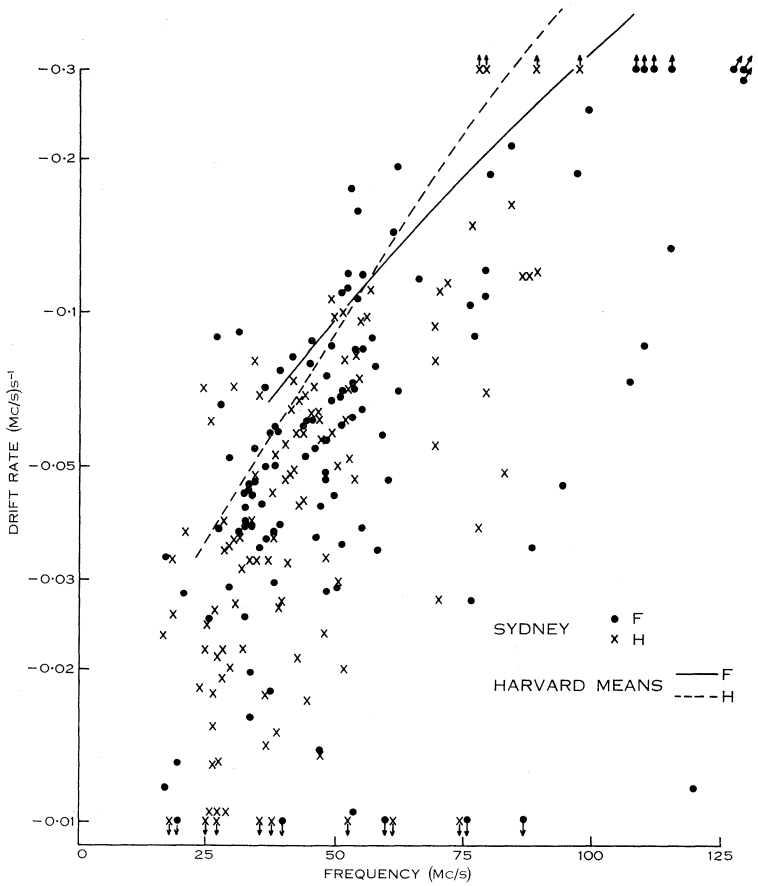

Fig. 1.—Scatter diagram of frequency drift rates for 21 type II bursts observed at Sydney. Each point represents a drift rate for an individual burst feature. Drift rates for harmonic bands have been reduced to the fundamental frequency assuming a harmonic ratio of two. The full and broken lines are mean drift rates for fundamental and harmonic (reduced to fundamentals) in a similar scatter diagram prepared by Maxwell and Thompson (1962) for type II bursts observed at the Harvard Radio Astronomy Station.

derived velocities, are identical with true source velocities only if the source propagates radially along the axis of the coronal streamer. The relation between derived and true velocities for non-radial propagation is examined in Section II(c). For our density model we choose, firstly, densities twice those given by Newkirk (1961) for the axis of an average optical coronal streamer (1956–1958); the agreement of other radio measurements with this "$2N$" model has been discussed by the author elsewhere (Weiss 1963). The appropriate formulae are:

$$\left.\begin{aligned} f &= 3\cdot65\times10^{2\cdot16/r}, \\ v &= -1\cdot40\times10^{5}(r^{2}/f)(\mathrm{d}f/\mathrm{d}t), \end{aligned}\right\} \tag{1}$$

where f is in Mc/s, v in km/s, r is the distance from the centre of the Sun in units of solar radii, and time is in seconds. Using these formulae, the velocities plotted in Figure 2 are obtained. In view of the large scatter, not too much importance should be attached to the average curves given in Figure 2, but it should be noted that at

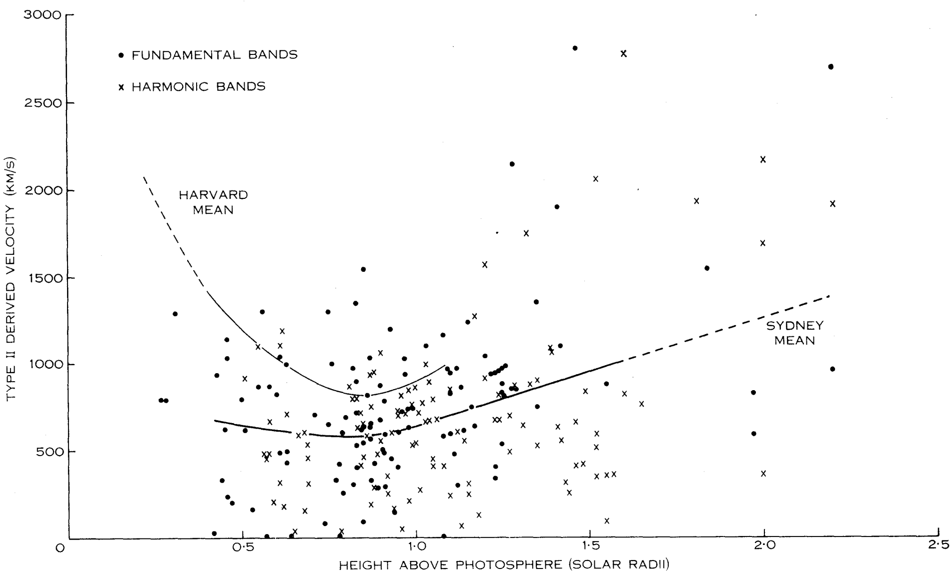

Fig. 2.—Scatter diagram of derived velocities of type II burst features derived from the frequency drift rates of Figure 1 assuming the $2N$ coronal density model. The line labelled "Sydney mean" is the average of the plotted points; that labelled "Harvard mean" is obtained from the Harvard mean curves in Figure 1.

all heights the average derived velocity exceeds both the local escape velocity and the speed of sound in the field-free corona (speed of sound for $T = 10^{6}$ °K is ~ 170 km/s).

Figure 3 gives the distribution of derived velocities, averaged over a height range $0\cdot4$–$1\cdot3\ R_{\odot}$ above the photosphere, for the 21 bursts. The scatter may be due to real differences in velocity from one burst to the next, or it may reflect variations in the physical conditions from one trajectory to the next or in the directions of propagation relative to the axes of the coronal streamers.

Figure 2 contains a suggestion, evident in both the average derived velocity and in the envelope of the cloud of points, that the type II source velocity increases with height at heights greater than 1 $R_{\odot}$. Although this is a statistical result, Figure 4 shows that the tendency for the derived velocity to increase with height is a real

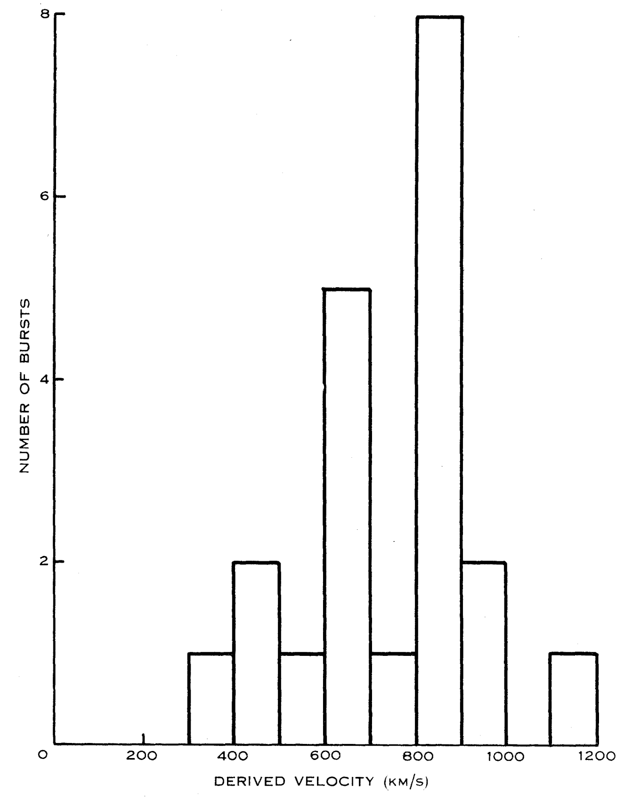

Fig. 3.—Histogram of derived velocities of 21 type II bursts, averaged over height range $0 \cdot 4$–$1 \cdot 3$ $R_{\odot}$ above photosphere.

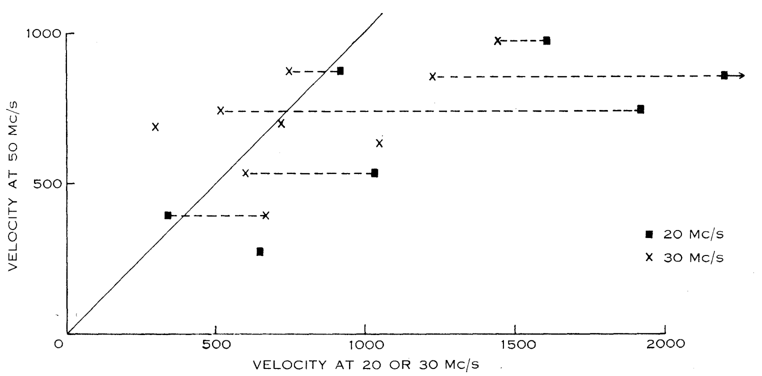

Fig. 4.—Comparison of type II source velocities (in km/s) at a height of $0 \cdot 90$ $R_{\odot}$ above the photosphere (corresponding to 50 Mc/s for the $2N$ density model) with velocities at heights of $1 \cdot 35$ and $1 \cdot 92$ $R_{\odot}$ (corresponding to 30 and 20 Mc/s). Dashed lines join pairs of points for the same bursts.

characteristic shared by the majority of bursts; moreover, the majority of the selected bursts discussed in part (*d*) below show an increase in velocity with height at the higher levels. At this stage, however, we should question whether the tendency for the derived velocity to increase with height is not one which is generated or enhanced by the particular density model, "2*N*", which has been chosen. As an alternative model, we may consider the $10\times$ Baumbach–Allen ("10BA") density law, as adopted by Maxwell and Thompson (1962) in their discussion of the Harvard

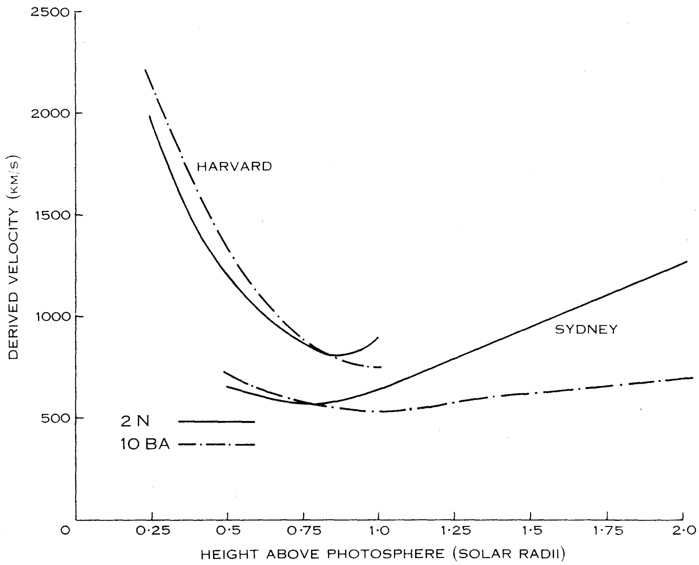

Fig. 5.—Average derived velocities for type II sources from $2\times$ Newkirk and $10\times$ Baumbach–Allen coronal density models.

velocity data; the 10BA model leads to considerably lower densities at great heights ($>2\,R_\odot$ above photosphere) than the 2*N* model. Formulae for the 10BA model are:

$$\left.\begin{aligned} f &= 285(1\cdot 55r^{-6}+2\cdot 99r^{-16})^{\frac{1}{2}}, \\ v &= -4\cdot 9\times 10^{3}\,\frac{(1\cdot 55+2\cdot 99r^{-10})^{\frac{1}{2}}}{9\cdot 3r^{-4}+47\cdot 8r^{-14}}\frac{\mathrm{d}f}{\mathrm{d}t}, \end{aligned}\right\} \tag{2}$$

where the symbols have the same meaning as in equation (1). Average derived velocities for this model are given in Figure 5; we see that for heights greater than $1\,R_\odot$ the tendency for velocity to increase markedly with height is no longer present.

The models upon which Figure 5 is based indicate that the behaviour of the derived velocity at greater heights ($>1\,R_\odot$ above the photosphere), and indeed whether the derived velocity increases or decreases with height, depends critically on the electron density model adopted. A simple argument, nevertheless, suffices to show that coupling of the observed frequency drift rates with any reasonable electron density model will lead to a derived velocity which does not decrease monotonically with increasing height. From Figure 1 we deduce that $(1/f)(\mathrm{d}f/\mathrm{d}t)$ $=\mathrm{d}(\ln f)/\mathrm{d}t$ decreases only slowly with decreasing frequency (by a factor of less than two over the frequency range 100–20 Mc/s, corresponding to a height range exceeding 1 $R_\odot$). Now it is a property of the exponential (static isothermal with constant gravity) model that the equation $(1/f)(\mathrm{d}f/\mathrm{d}t)$ = constant corresponds to constant velocity; hence, for this model a slight decrease in $(1/f)(\mathrm{d}f/\mathrm{d}t)$ with height implies a slight decrease in velocity with increasing height. Any reasonable density model which allows for the height-dependence of gravity and also for the possibility of outward flow of matter will fall off much more slowly with height than the static isothermal constant-gravity model and so lead, from the measured frequency drift rates, to velocities which increase, although perhaps slowly, with height. Velocities derived from two density models (10BA and 2*N*) have been examined. Of these models the 2*N*, which leads to substantially higher velocities at greater heights, is preferred because of support by other radio observations of source heights (Weiss 1963).

We may conclude, therefore, that with current coronal electron density models the most probable derived velocity for type II sources at heights near 1 $R_\odot$ above the photosphere is 750 km/s, and that at greater heights the derived velocity either remains constant or, more probably, increases slowly with height. The Harvard observations (Maxwell and Thompson 1962) suggest that in the lower corona the derived velocities increase rapidly to some 1500 km/s or more. The Harvard result, however, is based on a small number of bursts, and does not seem to be supported by the Sydney observations which indicate essentially constant average velocity over the height range 0·4–1·0 $R_\odot$.

(c) *Significance of the Derived Velocities*

In the last section frequency drift rates have been converted into derived velocities using an electron density law appropriate to the vertical axis of a coronal streamer. The derived velocity can therefore be identified with the true source velocity only if the type II source propagates along the axis of the streamer. Positional data, however, suggest that for a small proportion of type II bursts the direction of propagation of the source is markedly non-radial in the heliocentric sense, and that for the great majority of bursts the inclination between the type II source trajectory and the axis of the coronal streamer (assumed radial) is less than 45° (Weiss 1963). Non-radial propagation appears to be sufficiently common to warrant investigation of the relation between the derived velocity and the true velocity of the source. Because of the structure of the coronal condensation this relation is neither simple nor self-evident; in particular, the derived velocity is not simply the radial component of the true velocity.

The relation between derived and true velocities has been examined using the model of a coronal streamer proposed by Newkirk (1961); the streamer has a Gaussian cross section whose width as a function of height is given in Table 2 of Newkirk's paper. The ratio (derived velocity/true velocity) is found to increase with height from the photosphere to a height $\sim 1\ R_\odot$; at still greater heights the derived velocity exceeds the true velocity by a factor which is independent of height but which depends on the inclination of the trajectory to the axis of the coronal streamer (assumed vertical) and on the electron density. The ratio (derived velocity/true velocity) may become quite large at heights exceeding 1 $R_\odot$; for example, for inclinations between 15° and 30° in a streamer of twice the density of the average streamer (1956–1958) this ratio is greater than $1 \cdot 6$. In general, however, one would expect this ratio to be much less than $1 \cdot 5$. Recalling that this velocity ratio is independent of height above 1 $R_\odot$, we note that the observed increase in derived velocity with height above this level, discussed in the last section, will be characteristic of the true velocity also.

The directions of propagation of individual type II sources are unknown. Thus there is no way of estimating true velocities of individual sources and hence, as suggested earlier, differences in direction of propagation of individual sources may contribute to the scatter in the derived velocities. In what follows, we shall assume that the derived velocity is in fact identical with the true velocity. On the average, we may expect this assumption to result in a slight overestimate of the true velocities.

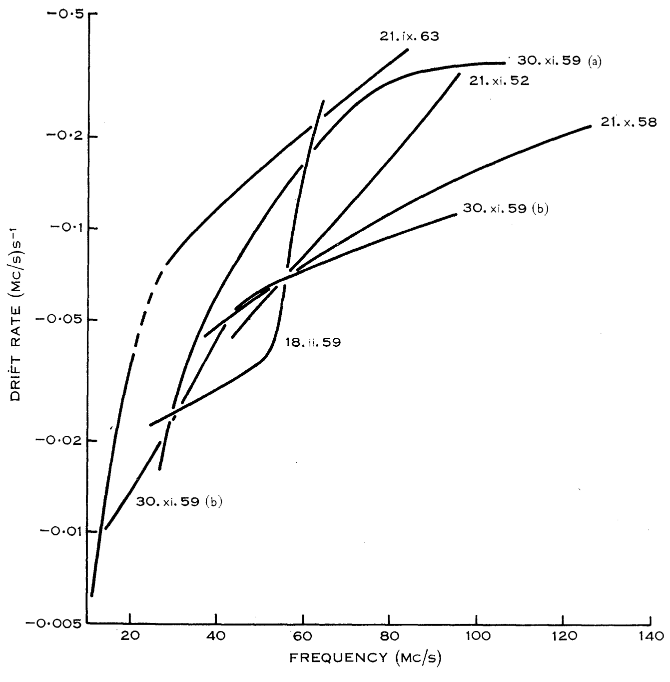

Fig. 6.—Smoothed rates of frequency drift for individual type II bursts. The burst of November 30, 1959 consisted of two main bands with incompatible drift rates; both bands are shown.

(*d*) *Data for Individual Bursts*

The large scatter of the individual points in Figures 1 and 2 raises the possibility that the concept of the "average" velocity of type II sources may be physically meaningless. It was therefore thought desirable to examine some individual bursts with well-defined structure extending over a wide frequency range. Frequency drift rates, harmonic ratios, and frequency separation of split bands for five such bursts are plotted in Figures 6 and 7. When reducing these bursts, minor irregularities and diffuse features were ignored, so that the data given in Figures 6 and 7 can be expected to furnish estimates of smoothed physical conditions appropriate to the sources (or groups of closely related sources if multiple bands are present) generated by the five individual flares. In one case (November 30, 1959) the drift rates and harmonic ratios for different bands proved to be incompatible; data for both bands have been retained in the subsequent analysis.

Figure 8 gives derived velocities as a function of height, assuming the $2N$ coronal density model. A previous warning should be repeated here, that these velocities have been obtained indirectly, by converting drift rates into velocities using the density model for the average coronal streamer, and since individual

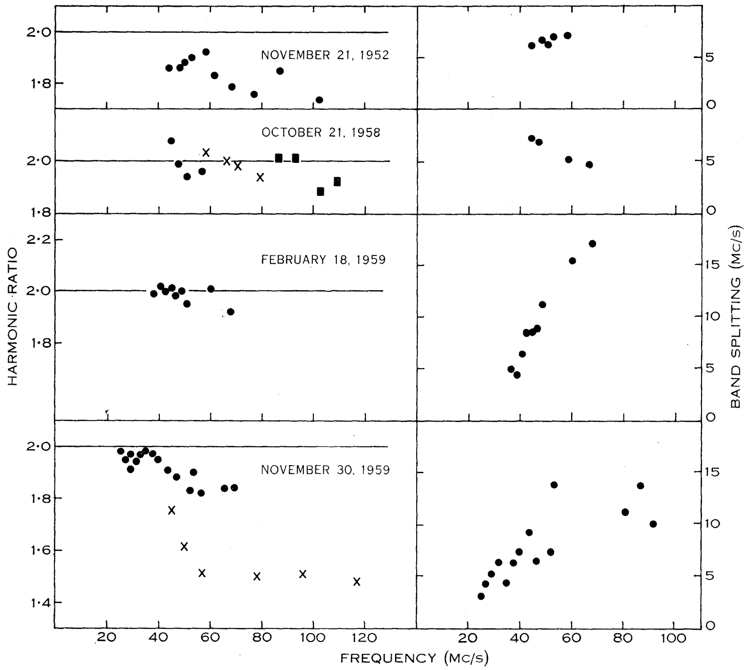

Fig. 7.—Harmonic ratios and frequency separation of split bands for individual type II bursts. Bursts of October 21, 1958 and November 30, 1959 were multiple, and harmonic ratios for different bands are distinguished.

streamers may depart from the average to an unknown extent, large errors in the derived velocities are possible. Figure 8 suggests that individual events do differ considerably, although it is impossible to say whether the differences lie in the true velocities, or in the structure of the streamers, or in the direction of the trajectory relative to the axis of the streamer.

Harmonic ratios (Fig. 7) are in most cases somewhat less than two, in agreement with the results of previous workers (Roberts 1959; Wood 1961; Maxwell and Thompson 1962). In all cases where adequate frequency range is available the harmonic ratios tend to increase (toward an upper limit very close to $2 \cdot 0$) with decreasing frequency. There is also a suggestion that different disturbances associated with the same flare may give systematically different harmonic ratios; this is particularly evident for the burst of November 30, 1959, and the event of October 21, 1958 appears to consist of three distinct disturbances, each with slightly different harmonic ratios at a given frequency. Apart from the low harmonic ratios, apparently exceptional, given by one band of the November 30, 1959 burst, the harmonic ratios are sufficiently close to $2 \cdot 0$ to warrant the assumption in Section II(a) of a ratio of exactly two when reducing drift rates for harmonic bands to fundamental frequencies.

Band splitting is of the same order as that reported by Roberts and by Maxwell and Thompson. The amount of band splitting δf increases steadily with frequency. By combining data for four bursts (Fig. 7) it is estimated that

$$\delta f = 1 \cdot 1 + 0 \cdot 124 f \qquad \text{(Mc/s)}.$$

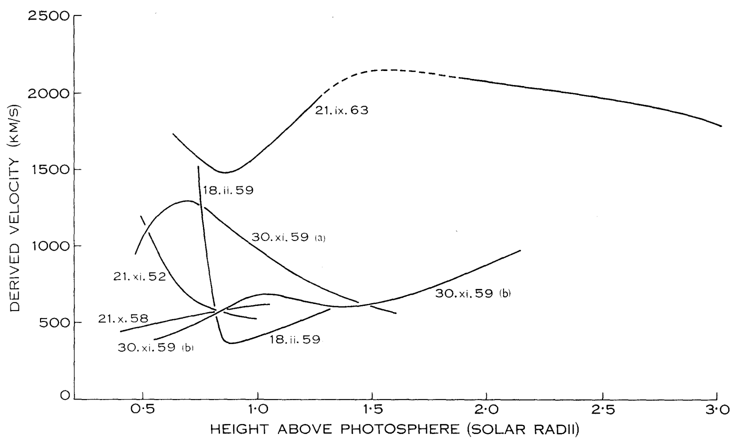

Fig. 8.—Derived velocities for individual type II bursts, assuming the $2N$ coronal density model.

III. Type II Velocities and Geomagnetic Cloud Velocities

It is of interest to compare the type II source velocity with the Sun–Earth travel time of the associated geomagnetic cloud. Because of the well-known difficulties in unambiguous association of geomagnetic storms with solar flares, comparisons of velocities were not possible for more than half the bursts. For identification purposes we have relied upon the "List of solar-terrestrial relationships IGY–IGC" prepared by Maeda *et al.* (1962). The data, plotted in Figure 9, indicate that the derived velocity of the type II disturbance is approximately equal to the average velocity of the associated geomagnetic cloud between Sun and Earth. Although this result substantiates a conclusion reached earlier by Hartz (1959) and by Moiseev (1960) using single-frequency radio data, it should be remarked here that, if the type II disturbance is a shock, there is no compelling reason to expect that its velocity over a limited range of coronal heights should be exactly or even approximately equal to that of the geomagnetic storm cloud (perhaps also a shock) in interplanetary space.

IV. Interpretation

In interpreting the foregoing data the plasma hypothesis for type II bursts will be adopted, i.e. that a flare-initiated disturbance moves outwards through the corona, generating electromagnetic emission of steadily decreasing frequency as it moves through regions of decreasing electron density. The evidence for this hypothesis, which has already been tacitly applied in converting frequency drift rates into velocities, has been reviewed recently by Wild, Smerd, and Weiss (1963). For our purposes it is not necessary to assume that the radiation originates in plasma waves which are subsequently converted into electromagnetic radiation. We require merely that the peak intensity of electromagnetic emission be generated at a frequency close to the local plasma frequency, so that it is legitimate to use a standard electron density model to convert frequencies into heights.

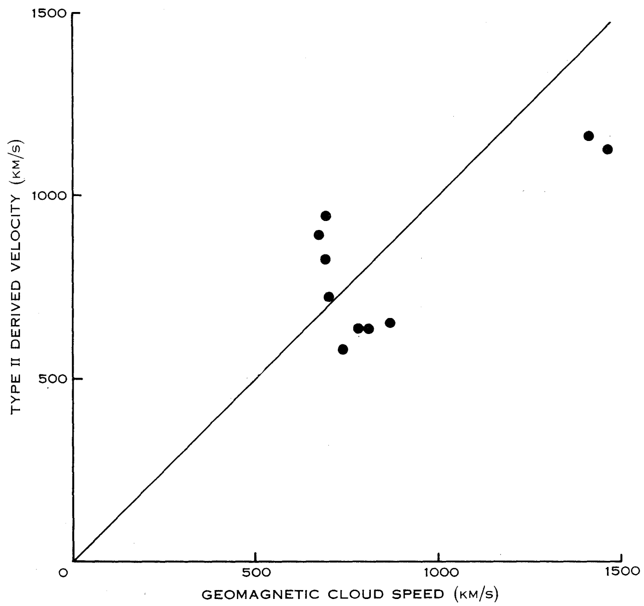

Fig. 9.—Comparison of derived velocities of type II sources (over height range $0 \cdot 4$–$1 \cdot 3\, R_{\odot}$ above photosphere) with average Sun–Earth velocities of associated geomagnetic clouds.

(*a*) *Theory of Shocks*

The speed of the type II disturbance exceeds the speed of sound in the field-free corona and we shall assume that the disturbance is a shock front. The common occurrence of narrow-band features in type II bursts then suggests that the shock width must be small. The long mean free path of fast ($\sim$ 1000 km/s) protons in the corona seems to preclude an ordinary collision shock, such as the shock occurring in a neutral gas, in which the structure of the shock front is determined by the collisional mean free path through viscosity and thermal conductivity measurements (Petschek 1958; Uchida 1960). The theory of shock waves in a fully ionized plasma is complicated and incomplete, but there appear to be at least two microscopic processes by which an irreversible dissipation of energy can take place across a narrow region and so produce a shock. These processes involve either electrostatic or electromagnetic couplings between electrons, ions, and fields. If no magnetic field is present or if the propagation of the shock is parallel to the magnetic field, electrostatic coupling may produce a shock whose width is of the order of a few times the mean free path of thermal particles in the undisturbed plasma; when magnetic coupling is the favoured process, then for propagation perpendicular to or oblique to the magnetic field the shock width is of the order of, or less than, the ion gyro radius (Gardner *et al.* 1958; Petschek 1958). Regardless of the nature of the microscopic process responsible for the increase in entropy across the shock, the Rankine–Hugoniot equations will apply provided that equilibrium is established amongst the particles behind the shock front.

The expected thickness Δ_{NM} (cm) of the non-magnetic shock has been calculated by Tidman (1962). From Figure 3 of his paper we have $\Delta_{\mathrm{NM}} \sim 2\times10^{16}N^{-1}$ for a temperature of 10^6 °K and Mach number $M = 2$. With electron density $N = 2\times10^7$ cm^{-3}, corresponding to a height of 1 $R_\odot$ in the $2N$ density model, $\Delta_{\mathrm{NM}} \sim 10^4$ km. This is much larger than the characteristic thickness Δ_{M} of the magnetic shock, for which $\Delta_{\mathrm{M}} \lesssim Mcv/eH \sim 10^{-4}v/H$ cm if v is the ion (proton) velocity in cm/s and H is in gauss. For $v = 1000$ km/s and $H = 1$ gauss, $\Delta_{\mathrm{M}} < 1$ km.

In situations where the magnetic field participates in the formation of the shock, the magnetic field strength is derivable from the observed properties of the shock. This situation may hold, for example, in the solar corona if the shock is strictly perpendicular to the magnetic field or has a substantial perpendicular component. Equations for the perpendicular magnetohydrodynamic shock are now well established (see, for example, Helfer 1953; Ferraro and Plumpton 1961). The following treatment describes a shock in a medium of infinite conductivity. The shock strength may be specified by the parameters

$$\eta = H_1/H_0 = \rho_1/\rho_0, \tag{3}$$

or

$$Y = p_1/p_0, \tag{4}$$

where H is the magnetic field strength, ρ the density, p the pressure, and the subscripts 0 and 1 refer to the undisturbed plasma and to the interior of the shock respectively. The relative importance of the magnetic field is specified by the parameter

$$Q_0 = H_0^2/8\pi p_0, \tag{5}$$

which is the ratio of magnetic to gas pressure. The Rankine–Hugoniot equations become

$$u_1/u_0 = 1/\eta; \qquad Q_1/Q_0 = \eta^2/Y;$$

$$Q_0(\eta-1)^3+\left\{\frac{2\gamma}{\gamma-1}+(Y-1)\right\}(\eta-1)-\frac{2}{\gamma-1}(Y-1) = 0, \tag{6}$$

where u is the velocity in a reference frame in which the shock is stationary. Equation (6) with $\gamma = 5/3$ has been explored numerically by Helfer. For our purposes it is more convenient to eliminate Y from (6) and from the equation for the shock speed V,

$$V^2 = \frac{a^2\eta}{\gamma(\eta-1)}\{(Y-1)+Q_0(\eta^2-1)\}, \tag{7}$$

to obtain

$$Q_0 = \frac{5}{\eta+5}\left(\frac{4-\eta}{3\eta}\cdot\frac{V^2}{a^2}-1\right), \tag{8}$$

where $a = (\gamma p_0/\rho_0)^{\frac{1}{2}}$ is the local speed of sound in the absence of a magnetic field. In deriving (8) we have taken $\gamma = 5/3$, although $\gamma = 2$ may be a more appropriate value for a magnetic shock in a tenuous plasma, when the component of velocity in a direction parallel to the magnetic field is a constant of the motion. If the shock is weak ($\eta \to 1$), we obtain from (8)

$$V^2 \sim a^2+H_0^2/4\pi\rho_0, \tag{9}$$

i.e. the shock speed is identical with the modified sound speed. The magnetic field strength can be deduced from (8) or (9) if the shock strength and speed are known. Equations (3)–(9), of course, apply to the non-magnetic shock if one puts $Q_0 = 0$. In particular, with $Q_0 = 0$ we obtain from (8) the relation between the Mach number $M = V/a$ and the shock strength η for the field-free case, that is

$$M^2 = 3\eta/(4-\eta). \tag{10}$$

The equations considered above apply to a one-dimensional stationary shock in a uniform medium. It is not immediately evident that they may be applied to type II bursts in the corona, where the density decreases rapidly outwards, the shock may spread laterally, and the strength of the shock is presumably reduced in time by dissipative processes. We may assume, however, that the shock equations apply locally, and consider the spreading through the energy equation. The available mechanical energy E in the shock front is given by:*

$$E \propto (R-R_0)^{\alpha}\rho_0 V^3\tau\nu(\eta-1)^2/\eta^2, \tag{11}$$

where $R-R_0$ is the distance in units of solar radii from the centre or plane of the shock, α is a coefficient whose value is 0 for a plane shock and 2 for a spherical shock, ν is a number whose value depends on, but is relatively insensitive to, the form of the shock front, and τ is a reduced time defining the steepness of the shock wave behind the front. Following Brinkley and Kirkwood (1947) and Uchida (1960) we shall take τ and ν to be invariant.

It is interesting to observe that under certain conditions equation (11) predicts qualitatively the outstanding feature of the observed dependence of derived velocity on increasing height, namely, a rapid initial decrease followed by a slower increase. For, if we assume E = constant and ignore changes in shock strength with time, (11) may be written, for a shock spreading spherically ($\alpha = 2$),

$$V = \text{const.}(R-R_0)^{-\frac{2}{3}}\rho_0^{-\frac{1}{3}}. \tag{12}$$

* This equation is valid irrespective of whether or not the shock is magnetohydrodynamic.

Values of V given by (12), normalized to $V = 1000$ km/s at $R = 2\,R_{\odot}$, are sketched in Figure 10 for the $2\times$Newkirk density model and for several values of R_0. For R slightly greater than R_0, we see that (12) is dominated by the rapid initial lateral expansion of the shock front, which produces a rapid decrease in V; at greater heights the importance of the expansion term is reduced, the density variation becomes dominant and leads to a slow increase in V. This behaviour is reminiscent of the derived velocities presented in Figures 2 and 5. Also, the curves in Figure 10 suggest that the large dispersion in derived velocities for individual events, particularly at heights less than $\sim 0\cdot 5\,R_{\odot}$ above the photosphere (see Fig. 8 of Maxwell and Thompson), may be attributed partly to variations in the value of R_0 from one burst to the next, i.e. the disturbances of different type II bursts may originate at different heights in the corona.

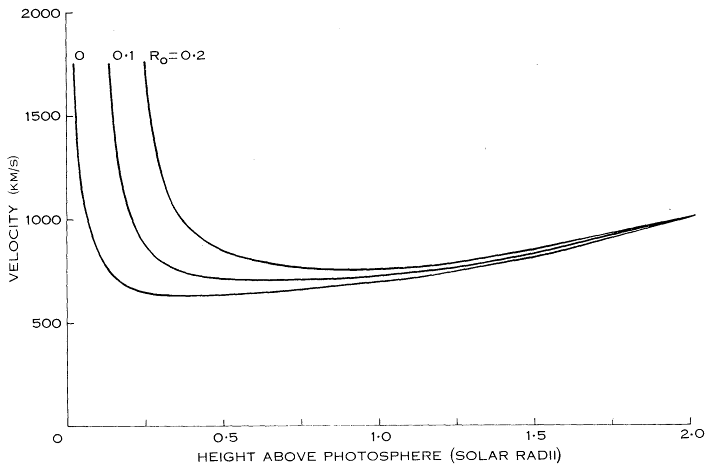

Fig. 10.—Source velocities predicted from the shock energy equation, on the assumption that the energy and shock strength remain constant and that the shock spreads spherically. R_0 is the height above the photosphere of the point of origin of the shock. Velocities are normalized to 1000 km/s at a height of $2\,R_{\odot}$.

The foregoing results differ radically from some numerical calculations by Uchida, who found that the shock speed is almost identical with the modified sound speed, and so is a monotonic decreasing function of height, over the whole of the height range examined by him ($< 1\,R_{\odot}$ above photosphere). The reason for this difference is that Uchida considered only dissipation of weak shocks, whereas we have considered spreading of a shock of arbitrary strength. It would be interesting to explore the behaviour of a shock in the corona subject to both spreading and dissipation; such calculations must await a satisfactory theory of the nature and strength of the type II shock, and of the dissipative process operating within it.

(b) *Test of Tidman's Theory*

Before considering the information on shock strengths and magnetic field strengths that is available in the data of Section II, we shall apply these data to the test of the ideas of Tidman, who suggested that fundamental and second-harmonic radiations are incoherent and arise in different regions, the fundamental in the undisturbed medium in front of the shock, the second harmonic in the denser medium within the shock. This theory connects the harmonic ratio to the shock strength parameter η through the relation $(f_H/f_F)^2 = \eta$. In order to obtain harmonic ratios $f_H/f_F \sim 2$, we require from (8) and (10) that the shocks be strong. For example, in the absence of a magnetic field, harmonic ratios of $1 \cdot 8$, $1 \cdot 9$, and $1 \cdot 95$ require Mach numbers $M = 3 \cdot 6$, $5 \cdot 3$, and $7 \cdot 6$ respectively; whilst for a perpendicular magnetic shock with $Q_0 = 4$ the appropriate values of M, still referred to the speed of sound in the absence of the magnetic field, are 10, 15, and 21 for $f_H/f_F = 1 \cdot 8$, $1 \cdot 9$, and $1 \cdot 95$ respectively and if $Q_0 = 10$ the corresponding values of M are 15, 23, and 32.

Inspection of Figures 7 and 8 shows at once that such large velocities are not observed for the bursts for which harmonic ratios have been measured, and we obtain from (8) negative values of Q_0 for all except one (November 30, 1959, part (*a*)) of the selected bursts. Thus, the shock strengths needed to account for the observed harmonic ratios would require shock speeds well in excess of the observed velocities, and we conclude that Tidman's theory is untenable, irrespective of whether or not the magnetic field is involved in the formation of the shock. This is not to deny the validity of Tidman's suggestion that type II emission may be connected with charge oscillations on a microscopic scale within the shock front; we assert merely that the present limited observational data are inconsistent with fundamental and harmonic emission arising in separate locations, i.e. in front of and within the shock front.

(*c*) *Shock Strengths and Magnetic Field Strengths*

Since Tidman's theory is untenable, we shall assume the alternative hypothesis, namely, that fundamental and second harmonic emissions originate at the same place through different scattering processes—Rayleigh scattering for fundamental, and combination scattering for second harmonic (Ginzburg and Zheleznyakov 1958; Smerd, Wild, and Sheridan 1962). In this event, for a non-magnetic shock, velocity and shock strength are simply related through (10). Using this formula and the derived velocities of Figure 5, we find Mach numbers in the range 3–8 and shock density ratios $3 \cdot 2$–$3 \cdot 8$. In the case of a magnetic shock, however, neither shock strength nor magnetic field strength can be determined directly from the available data. If the shock has no substantial component parallel to the magnetic field, only an upper limit to the field strength can be obtained, by assuming a weak shock and using (9). In the more general case of oblique magnetic shocks an upper limit to the field strength is found by equating the shock speed to the Alfvén velocity, thus,

$$H_{\max} = V(4\pi\rho_0)^{\frac{1}{2}}. \tag{13}$$

In the corona a (~ 170 km/s for $T = 10^6$ °K) is usually considerably less than the speeds of type II disturbances, and limiting magnetic field strengths derived from (9) and (13) do not differ appreciably. Field strengths found from (13) using the derived velocities of Section II (Sydney data, Fig. 5) are given in Figure 11. We have also shown in Figure 11 a critical (minimum) field strength, which has been taken as the field strength required to equalize magnetic and gas pressure in the average coronal streamer, i.e. $Q_0 = 1$ in (5). It is satisfactory that the fields derived from (13) decrease with increasing height and exceed the critical field by an adequate margin. It should be emphasized, however, that Figure 11 purports to give coronal magnetic field strengths only if the shock is neither parallel nor near-parallel to the field lines.

(*d*) *Magnetic Field Strengths from Band Splitting*

We turn finally to examine the magnetic theories of band splitting. If band splitting has a magnetic origin and the shock is also magnetic, we should expect magnetic fields derived from the two theories to be consistent. Two magnetic

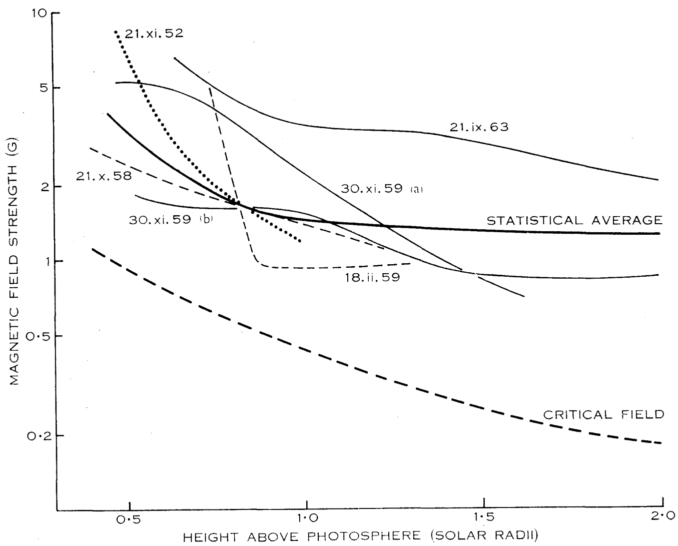

Fig. 11.—Coronal magnetic field strengths derived from the assumption that the type II disturbance is a perpendicular magnetic shock. The heavy full line is the upper limit to the field strength obtained by averaging over all bursts (velocities from Figure 2). The heavy broken line is the minimum field strength, for which gas pressure = magnetic pressure. The dated lines give upper limits for individual bursts (velocities from Figure 8).

theories of band splitting, neither entirely satisfactory, have been suggested. In the first theory, the two frequencies in the split bands correspond to frequencies at which the refractive index vanishes in a magneto-ionic plasma. The frequency separation δf is given by:

$$\begin{aligned}\delta f_{\mathrm{MI}} &= (f_0^2+f_{\mathrm{G}}^2)^{\frac{1}{2}}+\tfrac{1}{2}f_{\mathrm{G}}-f_0,\\ &\sim \tfrac{1}{2}f_{\mathrm{G}} \qquad (f_0 \gg f_{\mathrm{G}}),\end{aligned} \tag{14}$$

where f_0 is the plasma frequency and f_{G} the gyro frequency. This theory, however, is unable to account for all the observed features (see Roberts 1959). The second theory (Sturrock 1961) invokes preferential excitation of the two frequencies at the extremities of the band of plasma waves that propagate at different inclinations to the magnetic field; the separation is

$$\delta f_{\mathrm{S}} = (f_0^2+f_{\mathrm{G}}^2)^{\frac{1}{2}}-f_0$$

$$\sim \tfrac{1}{2}f_{\mathrm{G}}^2/f_0 \qquad\qquad (f_0 \gg f_{\mathrm{G}}). \tag{15}$$

Sturrock's theory presumably requires that the type II shock be sufficiently disordered that plasma waves are able to propagate isotropically. Magnetic field strengths derived from (14) and (15) using the data of Figure 7 are given in Figure 12. We have

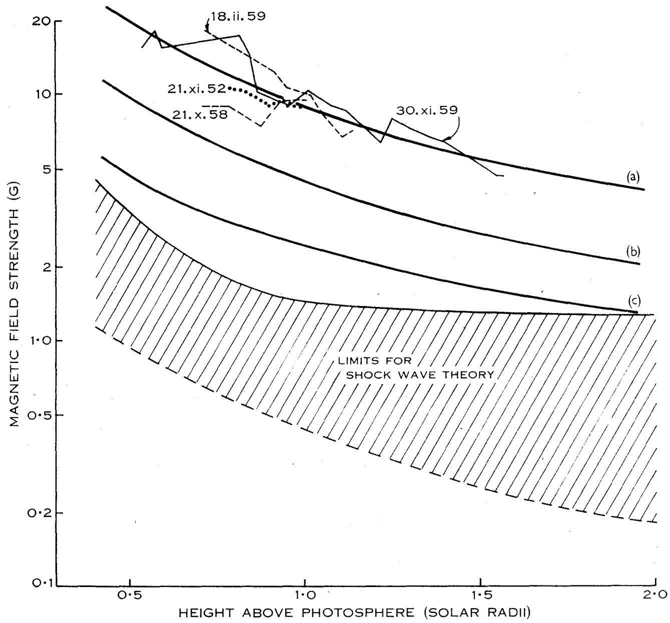

Fig. 12.—Coronal magnetic field strengths derived from band splitting of four individual type II bursts. The three heavy lines are the field strengths (averaged over these four bursts) according to (*a*) Sturrock's theory, (*b*) magneto-ionic splitting, (*c*) beating between plasma and gyro frequencies. The dated lines indicate scatter amongst the individual bursts. The shaded region reproduces from Figure 11 the band of average field strengths permissible for a magnetic shock.

also included the magnetic field strengths derived from these data using the assumption, for which there is admittedly little theoretical justification, that band splitting represents a beat phenomenon between plasma and gyro frequencies, so that

$$\delta f_{\mathrm{b}} = f_{\mathrm{G}}. \tag{16}$$

Detailed comparison of Figures 11 and 12 shows that, without exception, the field strengths derived from (14)–(16) are larger than the field strengths permissible if the shock is magnetic.

V. Discussion

We have examined, both statistically and for a few well-documented events, some features of type II bursts which are relevant to the problem of the nature of the sources of the bursts. The features examined include velocities, harmonic ratios, and band splitting; from them, assuming that the type II disturbance is a shock front, we have attempted to infer shock strengths and values of coronal magnetic field strength.

The derivation of the radial component of velocity is complicated by uncertainties in the electron density model appropriate to greater heights. The following conclusions, however, appear to be substantiated:

(i) On the average, derived velocities decrease from a value which may be as large as 1500 km/s near $0 \cdot 2\ R_{\odot}$ above the photosphere to a value ~ 750 km/s at a little below $1\ R_{\odot}$. Above this level the average velocity probably increases slowly with height. This behaviour is consistent with predictions from a simple form of the shock energy equation.

(ii) Scatter in derived velocities between and within bursts is large. This may be due to real scatter in the velocities, to non-radial propagation, or to structural differences between coronal streamers.

(iii) The velocities of type II sources, measured near the minimum velocity, agree well with the average Sun–Earth travel times of the associated geomagnetic storm clouds.

(iv) The source velocity exceeds the escape velocity at all heights, and also exceeds by a considerable margin the speed of sound in the field-free corona.

We have assumed, because of the close association between type II bursts, type IV bursts, and solar active regions, that a magnetic field is present in the coronal regions (e.g. in streamers) where type II bursts propagate. The present observations, unfortunately, do not allow us to decide whether or not the magnetic field participates in the formation of the type II disturbance. That the magnetic field is involved, at least in some cases, is strongly suggested by the occurrence of herring-bone structure; this structure in bursts with abnormally low, or zero, rate of frequency drift is very easily explained if the type II burst is a perpendicular magnetic shock (see Wild 1964). Without making a decision concerning the role of the magnetic field, we here summarize the inferences which can be drawn at the present time regarding the characteristics of the type II disturbance and the possible magnetic field strengths.

(1) The observed velocities and harmonic ratios are incompatible with the structure proposed by Tidman in which fundamental and second harmonic emissions arise respectively in front of and within the shock.

(2) *If the shock is non-magnetic,* electrostatic coupling dominating over magnetic coupling, the shocks are strong with Mach numbers in the range 3–8 and density ratios exceeding 3. Magnetic theories of band splitting indicate fairly strong fields (3–10 G at $\sim 1\ R_{\odot}$, depending on the theory adopted) which decrease with increasing height and exceed by factors of 6–20 the critical field strength required to support the average coronal streamer against diffusion.

(3) *If the shock is magnetic,* an upper limit to the magnetic field strength can be derived from shock theory. This maximum field exceeds the critical field by an ade-

quate but not generous margin (a factor of 4–8), but is smaller (by factors of 2–5 depending on the theory adopted) than the fields required by the magnetic theories of band splitting. The discrepancy between the two estimates of the field strength cannot be reconciled by rescaling the favoured (Newkirk) density model, since to obtain the desired increase in source velocity the density must be increased, and the densities adopted are already larger than those observed optically. The discrepancy is also too large to be resolved by any reasonable change in the form of the electron density model. The implication of the inconsistency in the derived magnetic field strengths is that, if the type II disturbance *is* a magnetic shock, the current magnetic theories of band splitting are untenable. We have already remarked that neither of these theories is entirely satisfactory. Maxwell and Thompson, by suggesting that band splitting originates in a double shock, have already raised the possibility of a non-magnetic origin for band splitting. However, the persistence of band splitting with almost constant temporal separation of the two ridges for many minutes and the sudden appearance and disappearance of the two bands at the same time, seem to preclude their explanation.

VI. Acknowledgments

The author is greatly indebted to Dr. J. P. Wild for criticisms and to Mr. S. F. Smerd for helpful discussions on the interpretation of the data. The considerable tasks of film measurement and reduction of observations were ably performed by Miss B. M. Hardwick.

VII. References

Brinkley, S. R., and Kirkwood, J. G. (1947).—*Phys. Rev.* **71**: 606.

Ferraro, V. C. A., and Plumpton, C. (1961).—"An Introduction to Magneto-Fluid Mechanics." Ch. V. (Oxford Univ. Press.)

Gardner, C. S., Goertzel, H., Grad, H., Morawetz, C. S., Rose, M. H., and Rubin, H. (1958).—Proc. 2nd UN Intern. Conf. on Peaceful Uses of Atomic Energy. Vol. 31, p. 230. (United Nations.)

Ginzburg, V. L., and Zheleznyakov, V. V. (1958).—*Astr. Zh.* **35**: 694. (English Trans. 1958: *Sov. Astron.* **2**: 653.)

Hartz, T. R. (1959).—IAU–URSI Symposium on Radio Astronomy, Paris, 1958. p. 554. (Stanford Univ. Press.)

Helfer, H. L. (1953).—*Astrophys. J.* **117**: 177.

Maeda, H., Sakurai, K., Ondoh, T., and Yamamoto, M. (1962).—*Annls. Géophys.* **18**: 305.

Maxwell, A., and Thompson, A. R. (1962).—*Astrophys. J.* **135**: 138.

Moiseev, I. G. (1960).—*Izv. Krymsk. Astrofiz. Obs.* **24**: 3.

Newkirk, G. (1961).—*Astrophys. J.* **133**: 983.

Petschek, H. E. (1958).—*Rev. Mod. Phys.* **30**: 966.

Roberts, J. A. (1959).—*Aust. J. Phys.* **12**: 327.

Smerd, S. F., Wild, J. P., and Sheridan, K. V. (1962).—*Aust. J. Phys.* **15**: 180.

Sturrock, P. A. (1961).—*Nature* **192**: 58.

Tidman, D. A. (1962).—*Phys. Fluids* **5**: 1104.

Uchida, Y. (1960).—*Publ. Astr. Soc. Japan* **12**: 376.

Weiss, A. A. (1963).—*Aust. J. Phys.* **16**: 240.

Westfold, K. C. (1957).—*Phil. Mag.* **2**: 1287.

Wild, J. P. (1964).—A.A.S.–N.A.S.A. Symposium on the Physics of Solar Flares. (Ed. W. N. Hess.) pp. 161–77. (N.A.S.A.: Washington.)

Wild, J. P., Smerd, S. F., and Weiss, A. A. (1963).—*Ann. Rev. Astr. Astrophys.* **1**: 291.

Wood, Marion B. (1961).—*Aust. J. Phys.* **14**: 234.